

Lab on a Chip

Accepted Manuscript



This is an *Accepted Manuscript*, which has been through the Royal Society of Chemistry peer review process and has been accepted for publication.

Accepted Manuscripts are published online shortly after acceptance, before technical editing, formatting and proof reading. Using this free service, authors can make their results available to the community, in citable form, before we publish the edited article. We will replace this *Accepted Manuscript* with the edited and formatted *Advance Article* as soon as it is available.

You can find more information about *Accepted Manuscripts* in the [Information for Authors](#).

Please note that technical editing may introduce minor changes to the text and/or graphics, which may alter content. The journal's standard [Terms & Conditions](#) and the [Ethical guidelines](#) still apply. In no event shall the Royal Society of Chemistry be held responsible for any errors or omissions in this *Accepted Manuscript* or any consequences arising from the use of any information it contains.

ARTICLE

A Novel Picoliter Droplet Array for Parallel Real-time Polymerase Chain Reaction Based on Double-inkjet Printing

Cite this: DOI: 10.1039/x0xx00000x

Yingnan Sun,^a Xiaoguang Zhou^{a,b} and Yude Yu*^{a,b}

Received 00th January 2012,

Accepted 00th January 2012

DOI: 10.1039/x0xx00000x

www.rsc.org/

We developed and characterized a novel picoliter droplet-in-oil array generated by a double-inkjet printing method on a uniform hydrophobic silicon chip, specifically designed for quantitative polymerase chain reaction (qPCR) analysis. Double-inkjet printing was proposed to efficiently address the evaporation issues of picoliter droplets during array generation on a planar substrate without the assistance of a humidifier or glycerol. The method utilizes piezoelectric inkjet printing equipment to precisely eject a reagent droplet into an oil droplet, which had first been dispensed on a hydrophobic and oleophobic substrate. No evaporation, random movement, or cross-contamination was observed during array fabrication and thermal cycling. We demonstrated the feasibility and effectiveness of this novel double-inkjet method for real-time PCR analysis. This method can readily produce multivolume droplet-in-oil arrays with volume variations ranging from picoliters to nanoliters. This feature would be useful for simultaneous multivolume PCR experiments aimed at wide and tunable dynamic ranges. These double-inkjet-based picoliter droplet arrays may have potential for multiplexed applications that require isolated containers for single cell cultures, single molecular enzymatic assays, or digital PCR, and provide an alternative option for generating droplet arrays on planar substrates without chemical patterning.

Introduction

Isolated microdroplets in an oil phase have great potential for use in chemical and biological research:¹ they can form microreactors in which reactions are isolated by the oil phase, which prevents cross-communication between droplets; they are monodisperse and therefore suitable for quantitative studies; and their ease of formation in quantity and extremely small volumes offer the possibility of manipulating single cells or molecules for high-throughput screening experiments. Many biochemical reactions have been successfully executed in single droplets.²⁻⁴ Notably, parallel polymerase chain reactions (PCR) in nano- to picoliter-sized microdroplets⁵⁻⁸ have garnered intense research interest in the past few years.

Various channel-based flow-through microfluidic systems have been developed to generate high-throughput emulsion microdroplets using T-junctions⁹⁻¹¹ or flow-focusing devices¹² at rates up to ~10 kHz. However, emulsion microdroplets generated from microfluidic channels are limited with respect to *in situ* monitoring. In another approach¹³, chambers with solid microcavity arrays have been used as microreactors in which droplets are separated by solid walls. These simple arrays have been successfully applied to quantify low-copy proteins in single cells¹⁴⁻¹⁷ and for on-chip PCR¹⁸⁻²⁰. However, the microfabrication is often time-consuming and expensive, and access to individual chambers and the manipulation of the

contents are difficult.²¹ Finally, any reuse of the microfluidic chip runs the risk of cross-contamination between samples.

In contrast to microdroplet generation under constant flow in microchannels or on microwell chips, recently developed techniques for the generation of droplet arrays (in micro- or even picoliter volumes) on planar substrates have set the stage for the direct manipulation of individual droplets, such as for image acquisition and quantification. A droplet array on a planar substrate has several advantages over the previous solid-walled pico- or nanoliter chambers.²¹ Because each droplet is isolated by oil, an individual droplet with its biological or chemical contents can be readily accessed. One important aspect of this feature is the ability to recover the droplet contents, which may be useful for further downstream analysis or processing. For example, an accessible droplet array was used as effective containment for cell culture.²¹ Since Guttenberg *et al.* first realized a planar chip device for PCR,²² planar droplet-based PCR has been utilized for various applications such as gene expression analysis²³ and the study of single cell methylation.²⁴ In addition, the effects of small volumes in PCR have also been investigated, and PCR performance has been evaluated by specifically examining the adsorption of reagents at the oil/water interface.²⁵ Most of the studies have used micropipettes to obtain regular droplet arrays with volumes in the hundreds of nanoliters under an oil layer in a Petri dish²⁶ or on a hydrophilic-in-hydrophobic-patterned

chemically modified substrate.^{21,24,27,28} Contact printing²⁶ and inkjet printing²⁹ have also been exploited and applied to high-throughput drug screening or enzymatic assays through the generation and precise control of droplet volumes. However, these approaches have several unavoidable problems. First, micropipette-based sampling arrays suffer from large droplet volumes and, therefore, low droplet densities. Second, droplet arrays formed on planar substrates generally require photolithographic masking of the chemically structured surface with a hydrophilic-in-hydrophobic pattern,^{21,24,27,28} thus requiring time-consuming semiconductor fabrication processes. Furthermore, the volumes of the formed microreactors cannot be easily changed.

The current inkjet-printing approach for picoliter or sub-nanoliter droplet generation can circumvent the above problems, but it suffers an intractable issue with droplet evaporation. To address this problem, some specific strategies have been devised, including the introduction of a medical nebulizer driven by compressed air or an ultrasonic humidifier while a droplet array is being printed,^{26,28} or deposition of reagents in nanoliter glycerol droplets²⁹ to maintain constant water content in the drops. However, the humidification approach runs the risk of cross-contamination when reagent droplets are exposed to the humidified air during printing. Furthermore, the addition of glycerol limits the useable types of bio-reagents, which are typically not compatible with PCR.

In this work, we developed and characterized a novel double-inkjet printing method to generate multiple droplet-in-oil arrays from pico- to nanoliter volumes on uniform silanized silicon chips, specifically designed for quantitative PCR. Shown schematically in Fig. 1, the double-inkjet printing technique uses piezoelectric inkjet printing equipment to first generate oil droplets of specified volumes on a planar substrate and then precisely deliver the amount of reagent into the oil droplets by jet action. This method affords several significant advantages over previous droplet array formation approaches. (1) The double-inkjet process vastly reduces the evaporation of reagent droplets during array fabrication. (2) There is no cross-contamination since reagent droplets are not exposed to air during printing. (3) This approach allowed open-access manipulation of the contents and multiple reagent injections into existing droplets. (4) The double-inkjet printing method could also serve as a contact-free sample loading method for programmable digital microfluidics based on electrowetting, which could help in generating large scale digital microfluidic droplets prior to parallel manipulation.³⁰⁻³³ In addition to the aforementioned advantages of double-inkjet printing, this method also shares the following advantages with the inkjet method: (1) Extremely high throughput and low sample consumption can be achieved due to the ability of the inkjet printing technique to dispense 1–10 pL droplets with high speed and positional accuracy. (2) There is no need for the complicated microfabrication of a patterned hydrophilic-in-hydrophobic surface. (3) Droplets with varying sizes and densities can be obtained at will during microreactor formation. In this paper, we first demonstrate the feasibility of double-

inkjet droplet formation and then evaluate the efficiency and reliability of this approach. Furthermore, we address droplet preservation by sealing to withstand elevated temperatures during thermal cycling, and successfully perform standard real-time PCR for the human 18S rRNA cDNA.

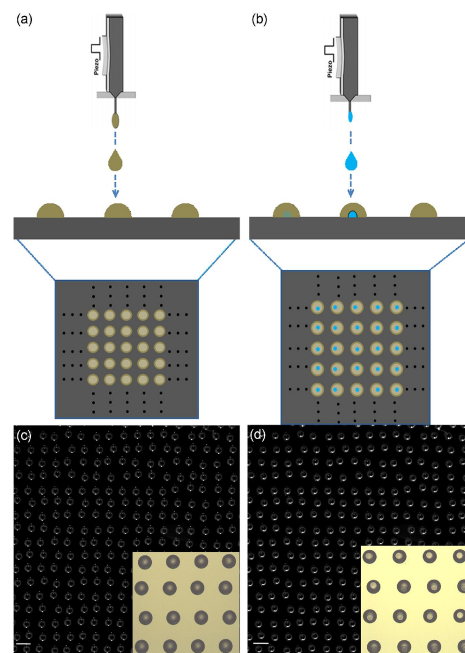


Fig. 1 Schematic representation and bright-field images of picoliter droplet-in-oil array fabrication by double-inkjet printing on a silicon dioxide solid support. (a) Oil droplet array formation. (b) The PCR mixture is dispensed on the first oil microarray to produce the droplet-in-oil array. The lower portions of (a) and (b) show top views of the oil and droplet-in-oil arrays. (c) Bright-field stereomicroscopic image of oil array on silica substrate. Inset: expanded view. (d) Bright-field stereomicroscopic image of droplet-in-oil array as fabricated in (b). Inset: expanded view. Scale bars: 500 μm .

Experimental

PCR droplet-in-oil array based on double-inkjet printing

All droplet-array generation was performed on a Jetlab[®] 4 inkjet platform (MicroFab Technologies Inc., USA) equipped with task-specific nozzles. Inkjet printing has been successfully demonstrated with this platform in a wide range of industries and applications.³⁴ The nozzle orifice diameters were 30 and 50 μm for reagent and oil droplet formation, respectively. Since the droplet volume is dependent on solution properties such as viscosity and surface tension, the piezoelectric pulse and voltage parameters were set according to the manufacturer's recommendations specific to the nozzle in order to obtain reproducible and stable droplet volumes. The inkjet dispensing process was monitored via stroboscope.

In this work, mineral oil (M8410, Sigma-Aldrich, 0.82–0.88 g/mL) was deposited on a silanized silicon dioxide surface using a 50 μm nozzle (MJ-AT-01-50, MicroFab) in a pattern created under computer control. Droplets containing the PCR reagent were printed on top of the oil droplets in the same pattern but with a nozzle 30 μm in diameter (MJ-AT-01-30, MicroFab).

To prevent adsorption of the PCR reagents onto the silicon surface,³⁵ a 600 nm layer of SiO₂ was grown on the silicon wafer by thermal oxidation at 1100°C for 2 h. Then, a rectangular area (2.7 cm × 1.6 cm) of the SiO₂ layer was gas-phase silanized in a desiccator with 1H,1H,2H,2H-perfluorooctyltriethoxysilane (Sigma-Aldrich) for 1 min at 85°C, to impart hydrophobic and oleophobic properties to the surface. Thereafter, droplet-in-oil arrays were printed in a 20 × 20 spot format with spot-to-spot spacings of 400 μm as shown in Fig. 1. The droplets-in-oil containing the PCR reagent created in this fashion were around 100 μm in diameter and approximately 800 pL in volume. Owing to the high-speed dispensing process, the printing of tens of thousands of droplet-in-oil spots on the same slide would be possible in just 10 min using a print-on-the-fly mode. The performance can be improved even more through further automatization and the development of multi-nozzle cartridges.

Chip packaging for sealing the droplet array

A chip package designed to preserve the reagent droplets for long-term operation at elevated temperature during thermal cycling is shown in Fig. S1. It consists of an array of disk-shaped droplets-in-oil on a silanized substrate, topped with a polydimethylsiloxane (PDMS) spacer to provide a squarish wall and create a tablet-like 10 mm × 10 mm chamber for the PCR reaction. The surface of the cover glass for the chip package was silanized in ethanol containing hexadecyltrimethoxysilane (10% v/v, Vetec™ reagent grade, 85%) at 70°C for 2 h to impart hydrophobicity. This helps to prevent the condensation of water vapor on the bottom surface of the cover glass.

After the droplet-in-oil array was formed through the double-inkjet printing technique according to the scheme in Fig. 1a and 1b, the array was gently overlaid with excess mineral oil (M8410, Sigma-Aldrich) via disposable pipette until the PDMS chamber was fully covered. Mineral oil was used because it is lighter than water (0.82–0.88 g/mL) and its solubility in water is extremely low.²⁸ Subsequently, the hydrophobic glass coverslip was placed on the PDMS spacer, effectively sealing the droplets of reagents under the oil layer without any fixed clamps.

Real-time PCR assay

The TaqMan® Fast Reagents Starter Kit, purchased from Life Technologies (Invitrogen Trading (Shanghai) Co., Ltd., China), is designed to detect and quantify eukaryotic 18S rRNA sequences in cDNA samples using the TaqMan 5'-nuclease assay in fast thermal cycling mode. This kit contains the TaqMan® Fast Real-Time Universal PCR master mix (2X), No AmpErase® UNG, eukaryotic 18S rRNA TaqMan® Assay (20X mix of two unlabeled PCR primers and a FAM™ dye-labeled 18S TaqMan® MGB probe) (Part Number 4331182), and human Raji cDNA. Each 20 μL PCR master mixture consisted of 10 μL TaqMan® Universal PCR master mix (2×, no UNG), 4 μL 18S rRNA (FAM dye) mix (20×), 1 μL Raji cDNA solution (diluted in Tris-EDTA (TE) buffer), 4 μL

RNase-free water, and 1 μL 50 mg/mL bovine serum albumin (BSA) solution. BSA was added to the PCR master mix as a blocking protein to occupy the adsorption sites at the water/oil interface and reduce the loss of polymerase from the bulk.³⁵ The negative controls contained RNase-free water in place of the cDNA solution. The starting concentration of the template DNA was 0.5 ng/μL. The concentration of the cDNA stock solution was determined using a NanoDrop spectrophotometer (Thermo Scientific).

Experimental Setup for qPCR-on-chip

A thermal cycling and fluorescence imaging system for real-time PCR-on-chip was developed by combining a homemade thermal cycler and an Olympus microscope. The homemade thermal cycler was controlled to perform temperature cycling during PCR using a PID temperature controller with LabVIEW software (National Instruments). Temperatures were calibrated with a thermocouple placed in the oil layer in the chamber. The PCR thermal cycles started with an initialization step of 10 min at 95°C to activate the enzyme. Next, a total of 40 cycles of amplification were performed as follows: a DNA denaturation step of 15 s at 95°C, a primer annealing step, and DNA extension step of 1 min at 60°C. The PCR products were stored in the cycler at 4°C before imaging.

The optical setup consisted of an Olympus microscope (TE2000, Olympus, Japan) equipped with a CCD camera (DP72, Olympus), a 5× objective lens (Olympus), a filter set of 460/20 nm for fluorescence excitation and 532/30 nm for emission collection of the FAM dye, and a filter set of 550/20 nm for excitation and 612 nm/long-pass for emission collection from the ROX dye. The ROX in the PCR reagent was used as a reference fluorescence signal to confirm the absence of volume changes in the droplets during thermal cycling. Green and red fluorescence images of the droplets were obtained in a 2000 μm × 2000 μm section at the end of each extension step for real-time PCR measurement. Additionally, 3D images were constructed by a confocal fluorescence microscope (ZEISS), and bright-field images of a large array obtained by a stereomicroscope and microscope.

All fluorescence images were converted into gray scale images, and the gray mean intensity of each droplet was measured using the ImageJ software program (NIH, USA). These values were then normalized, and the real-time PCR values were calculated.

Discussion

Double-inkjet method for droplet-in-oil array preparation

To prevent the evaporation of droplets during printing, a double-inkjet printing method was designed and applied to produce droplet-in-oil arrays. The principle of the double-inkjet printing for droplet-in-oil formation is schematically illustrated in Figure 1a and 1b. First, oil droplets (e.g., mineral oil) are dispensed piezoelectrically on a silanized SiO₂ substrate with excellent hydrophobic and oleophobic properties (Fig. 1a). Then, a second-pass printing of the aqueous reagent is carried out on top of the just-formed oil droplets (Fig. 1b). As the

velocity of the ejected droplets is as high as 3–5 m/s, the droplets carrying the chemical reagents will penetrate the oil droplets, overcoming their surface tension and viscosity. The aqueous droplets subsequently sink to the bottom of the less-dense mineral oil droplets, forming stable droplet-in-oil structures as shown in Fig. 1d. To obtain a large array of monodisperse droplet-in-oil structures, we aligned the inkjet nozzle with the oil droplets patterned on the substrate using the printer's control software and the two dimensional platform.

Optimization of droplet-in-oil formation

SURFACE PREPARATION Surfaces patterned with hydrophilic spots surrounded by hydrophobic areas have been prepared previously through photolithography and chemical modification.²⁸ They were used in the preparation of droplet arrays and the immobilization of droplets during thermal cycling. Different from these studies, we developed a silica wafer with a uniform hydrophobic and oleophobic surface on which to fabricate picoliter droplet-in-oil arrays via the double-inkjet printing method. This surface facilitated droplet-in-oil preparation and droplet immobilization during thermal cycling without noticeable volume or position changes.

We tested the idea of double-inkjet printing by fabricating a droplet-in-oil array of 20×20 spots with diameters of $100 \mu\text{m}$ or less and spot-to-spot spacings of $400 \mu\text{m}$ (Fig. 1c and 1d). The droplet-in-oil array was prepared on a silicon wafer with a thermal conductivity of $157 \text{ W/m}\cdot\text{K}$ to ensure efficient heat transfer and good thermal uniformity. Moreover, we grew a 600 nm layer of SiO_2 on the wafer for surface passivation since silica material was proven to be an enzymatic inhibitor for PCR.²¹ The optical properties of silicon dioxide also provided an impetus for its use, as silicon oxide surfaces show a lower mean gray value compared with the mean gray values of silicon surfaces.³⁶

After passivation, the silica chip was surface treated by silanization. We used this step for two reasons. First, in order to create oil droplets large enough to fully enwrap the reagent droplets, the oil drops had to be formed with higher contact angles and larger volumes. Consequently, we modified the substrate with a fluorosilane to increase its oleophobicity and facilitate ball-like oil droplets with larger contact angles. Optimum contact angles of 119.5° and 72.1° , respectively, for water and mineral oil were obtained (Fig. 2a and 2b). Furthermore, the increased contact angle of the oil allowed for more compact droplets with smaller intervals, increasing the droplet density of a given area. Second, the stabilization effect due to the higher reagent contact angle helped to keep the droplet-in-droplet array stationary during the dispensing of the overlaying oil into the reservoir and during PCR thermal cycling. The contact angle of the droplet was critical to its long-term preservation, especially its stability during thermal cycling. However, excessive substrate surface hydrophobicity is not conducive to the stability of the droplet array; even the slow overlaying of oil on the substrate surface could easily disrupt the array formation. Even if the droplet formation was maintained after application of the oil, the problem of long-term

preservation still remained; some droplets would easily float in the overlaying oil despite the greater density of the aqueous droplet (1.0 kg/m^3) compared to the mineral oil (0.8 kg/m^3). Therefore, to maintain a stable droplet-in-oil configuration, the extent of substrate surface silanization must take into account both the lipophobicity of the oil drops and the hydrophobicity of the reagent drops. The conditions for a stable double-inkjet-based droplet-in-oil preparation on a surface are dependent on the optimization of these parameters.

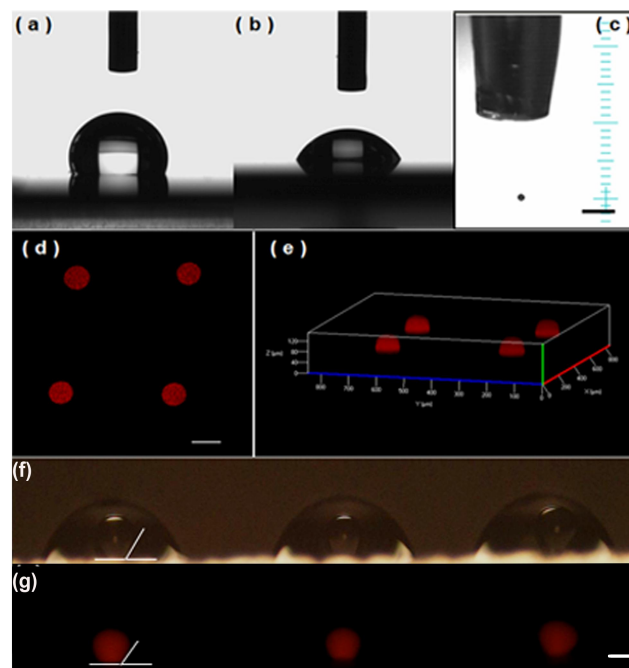


Fig. 2 (a) Contact angles for DI water and (b) mineral oil were 119.5° and 72.1° , respectively. (c) Stroboscopic image of a pinched-off droplet used to calculate the accurate volume and velocity. Scale bar: $500 \mu\text{m}$. (d) Top view and (e) 3D images of four droplets formed on a silicon glass slide. Images were taken by a confocal fluorescence microscope. Scale bar: $100 \mu\text{m}$. (f) Bright- and (g) fluorescence side-view images of droplet-in-oil structures taken by a microscope. Scale bar: $100 \mu\text{m}$.

DROPLET DYNAMICS Accurate analysis of droplet dynamics was carried out by stroboscopic imaging, which was included in the Jetlab printing platform (Fig. 2c). This analysis identified a second crucial parameter for double-inkjet printing that affects the final spot quality: the reagent droplet velocity at the moment of impact on the oil drop. Only a reagent droplet with sufficiently high incident energy was able to overcome the surface tension of the oil drop and achieve successful penetration. When the droplet velocity decreased below a critical value, the reagent droplet would slip from the impact site on the spherical oil drop to the side edge, rather than penetrate it. More details that illustrate the effects of the injection velocity on the double-injection process are shown in Movie S1 (ESI), and an entire double-inkjet printing procedure is shown in Movie S2 (ESI). Theoretically, during the impact, the kinetic energy of the reagent droplet transfers into the surface energy and viscous dissipation of the system. If the reagent droplet could not penetrate into the oil drop, after the

velocity of reagent droplet reaches zero, the surface energy transfers back to the kinetic energy of the reagent droplet to push it outwards. The reagent droplet will then float on the interface of the spherical oil drop. This unstable state will lead to the slipping of the reagent droplet eventually. In this study, all droplet-in-oil fabrication experiments were carried out at droplet velocities higher than 3–5 m/s at voltages around 30–50 V, resulting in 60–200 pL droplets as shown in Fig. S3.

Reliability of double-inkjet printing for droplet-in-oil arrays

Since the fluorescence intensity of the droplet constituted the integrated intensity of the entire droplet and the original concentrations of fluorescence reagents were the same, it could indirectly suggest the consistency of the volume of the droplet. To evaluate the accuracy and reliability of the double-inkjet method for droplet-in-oil generation, we investigated the fluorescence intensities of reagent droplets after the double-inkjet procedure. The relative standard deviation (RSD) of the

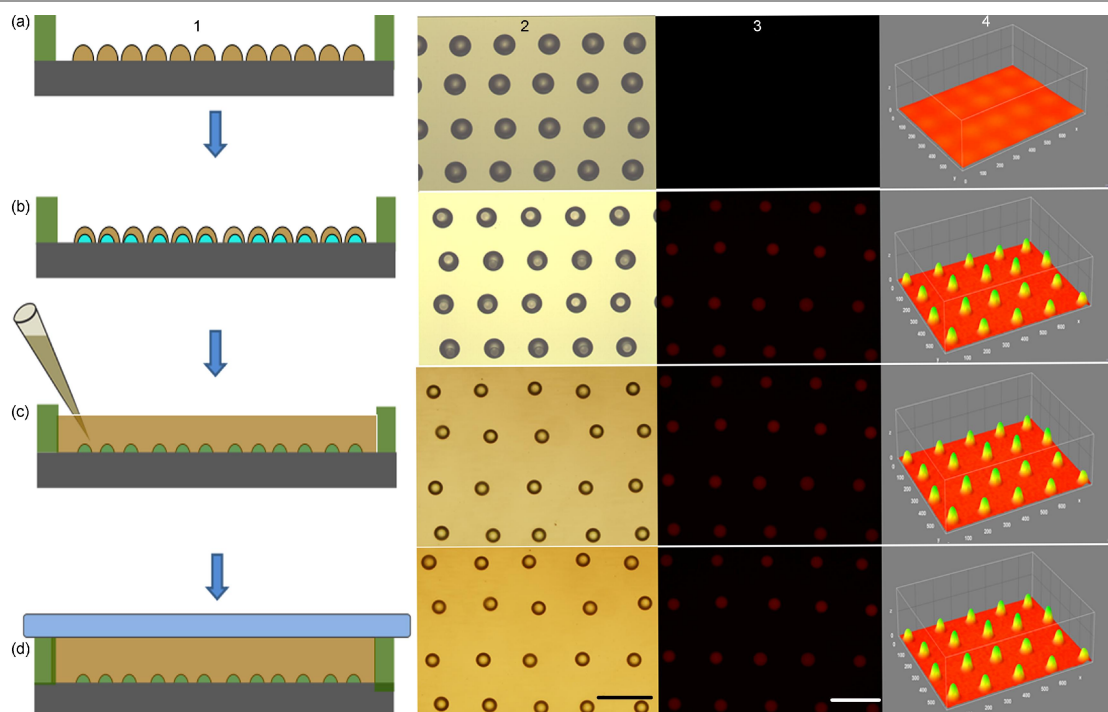


Fig. 3 Process schematic (column 1, a–d), bright-field microphotograph (column 2, a–d), fluorescence images (column 3, a–d), and their 3D surface plots (column 4, a–d) showing the whole formation procedure of a picoliter droplet array for PCR. In row (a), a 4×5 array was generated with 2 nL mineral oil droplets. Row (b) shows the same droplets after 800 pL PCR reagent containing ROX dye used as a passive reference was added into the oil droplets. In row (c), excess mineral oil was injected with via micropipette until the droplet array was wholly covered. Finally, in row (d), the chip after sealing with a coverslip was placed on thermal cycler to perform parallel real-time PCR for 40 cycles. Scale bars: 500 μm .

fluorescence intensity was measured to demonstrate the effectiveness of the method and the uniformity of the drop sizes. Figure 3 demonstrated the fluorescence images of droplet arrays dispensed through the double-inkjet procedure in volumes of 800 pL, specifically shown in Figure 3 (column 3). The RSD of the fluorescence intensities of 20 droplets covered in oil were within 7.8%, which is consistent with the results obtained from a continuous-flow-based droplet PCR platform,¹⁷ thus confirming both the reliability and robustness of the double-inkjet method.

To assess the double-inkjet method as an effective solution to prevent evaporation during droplet array fabrication, we first calculated and then contrasted the volumes of the reagent droplets before and after injection into oil drops to establish their consistency. Pre- and post-injection droplet volumes were measured by two independent techniques: stroboscopic imaging

in air and a wetting contact angle measurement on the surface surrounded by oil, respectively. Figure 2c presents a stroboscopic image showing the accurate volume of a droplet before impacting an oil drop. Using the 3D images shown in Figure 2d and 2e, we measured the droplets under the oil layer as having 90 μm diameters and calculated the contact angles and volumes accordingly, assuming that they formed partial spheres. Based on the comparison of the volumes of 100 reagent droplets, the coefficients of variation of these droplets with diameters of 80, 100, and 120 μm were less than 4, 5, and 4.7%, respectively. Consequently, we concluded that the final volume of a reagent droplet contained in an oil drop was basically equivalent to the actual volume of the pinched-off droplet exiting at the nozzle.

Next, we evaluated the long-term preservation of droplets-in-oil on the silanized plate. A fluorescent dye solution (ROX, ABI)

was double-inkjet printed in a 1×3 array of droplets with 700 pL volumes. We measured the volumes and fluorescence intensities of the droplets-in-oil after allowing them to stand for ~ 3 h at room temperature ($\sim 23^\circ\text{C}$). As shown in Fig. S2, no significant changes in spot morphology or fluorescence intensity were evident after an hour. This showed that the final droplets-in-oil would remain stable long enough to withstand the subsequent assembly time required for oil overlaying in the reservoir for long-term sealing. We also verified that the final droplet array sealed in the sandwiched chip structure was stable for at least 5 days. As shown in ESI Fig. S5, there were no obvious changes in the shape or fluorescence intensity of the droplet array sealed in the oil layer after standing at room temperature for 5 d. Many experiments could be carried out without considering the change in concentration, while the mean fluorescence intensities of the droplets increased by 2.0%. This would enable diverse applications, which require long-term monitoring, such as protein crystallization³⁷, cell proliferation³⁸, and immunoassays³⁹.

Another advantage of the double-inkjet method is its versatility in generating an array of droplets with varying volumes, especially for PCR applications. Instead of adjusting the driving pulse, the droplet volumes can be varied more simply: by setting the jet frequency (i.e., the number of droplets per pulse) via the software, achieving multiple droplet volumes by multiplying the incremental magnitude from pico- to nanoliter scale. The ability of the double-inkjet printer to fabricate droplets at varying volumes is evident from the volume gradient shown in Figure 4. This figure illustrates images of droplets ejected with jet frequencies of 2, 4, 6, and 8 Hz (bottom to top of figure), affording droplet volumes of 124, 248, 372, and 496 pL, respectively. Compared to previous methods for generating multivolume droplets, such as microstructures fabricated with semiconductor techniques, our approach has the advantages of high accuracy, flexibility, and convenience. This approach could prove to be valuable for multivolume PCR⁴⁰ experiments, affording wider and tunable dynamic ranges.

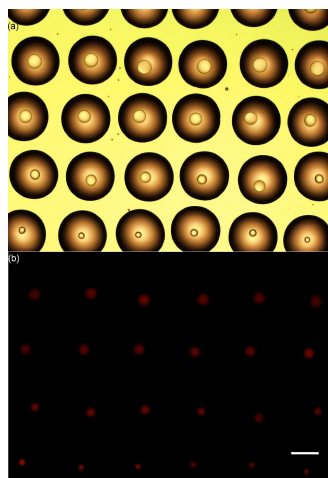


Fig. 4 (a) Bright and (b) fluorescence images of multivolume droplet-in-oil array. From bottom to top, droplets ejected at jet frequencies of 2, 4, 6, and 8 Hz. The

final droplet volumes were 124, 248, 372, and 496 pL, respectively. Scale bar: 250 μm .

Performance of picoliter real-time PCR-on-chip

We employed human Raji cDNA of 18S rRNA to test the performance of real-time PCR with serial dilutions of DNA template concentrations, using a droplet array fabricated by the double-inkjet procedure on a uniform silanized silica substrate. Figure 5a shows fluorescence images of droplets with 50 pg/ μL cDNA after different thermal cycles, and Figure 5b displays the characteristic real-time PCR profiles of droplets with serial dilutions of over five orders of magnitude (from 500 to 0.05 pg/ μL). The corresponding threshold cycle (C_t) values were 14.8, 17.5, 21.2, 24.4, and 27.8 for the series, along with a negative control that displayed no changes in fluorescence. These results were comparable with data obtained from a commercial real-time PCR system (Fig. S4, ESI), further proving the potential and effectiveness of this novel double-inkjet printing method for PCR experiments. It is also worth mentioning that the reagent consumption in our real-time PCR experiment was at least 120 times lower than in the conventional real-time PCR assays. Compared with microchannels and microwells, which were also picoliter-level (achieved through microfabrication), this method does not require the use of extra reagent fluid for flushing, and thus reduces the reagent consumption.

In this work, we demonstrated the feasibility of using double-inkjet printing and accomplished all the necessary steps to perform real-time PCR analysis in a droplet-in-oil array format. First, we effectively addressed the issue of picoliter droplet evaporation during thermal cycling and maintained a stable droplet structure on the uniform hydrophobic surface, by careful design of the chip and without any emulsifier. As shown in Fig. 3, there was no loss of fluorescence intensity of the ROXTM dye, no random movement of droplets on the uniform hydrophobic substrate, and no sample cross-contamination after 40 thermal cycles. Second, the successful PCR of each droplet suggested that the DNA-polymerase retained its enzymatic activity and viability after being printed onto the substrate through the double-inkjet procedure with appropriate jetting voltages in a certain range. Third, the real-time PCR performed in the double-inkjet-printed droplet array demonstrated high sensitivity and efficiency with a lower concentration DNA template. This suggests that single-molecule amplification could be possible with these double-inkjet-based droplet arrays, paving the way for performing digital PCR assays on this system.

Conclusion

We presented a method for the rapid generation of a picoliter droplet-in-oil array dispensed by piezoelectric double-inkjet printing on a uniform, hydrophobic, silanized substrate. By this

approach, we performed a parallel real-time PCR assay with comparative sensitivity and dynamic range (5 log range).

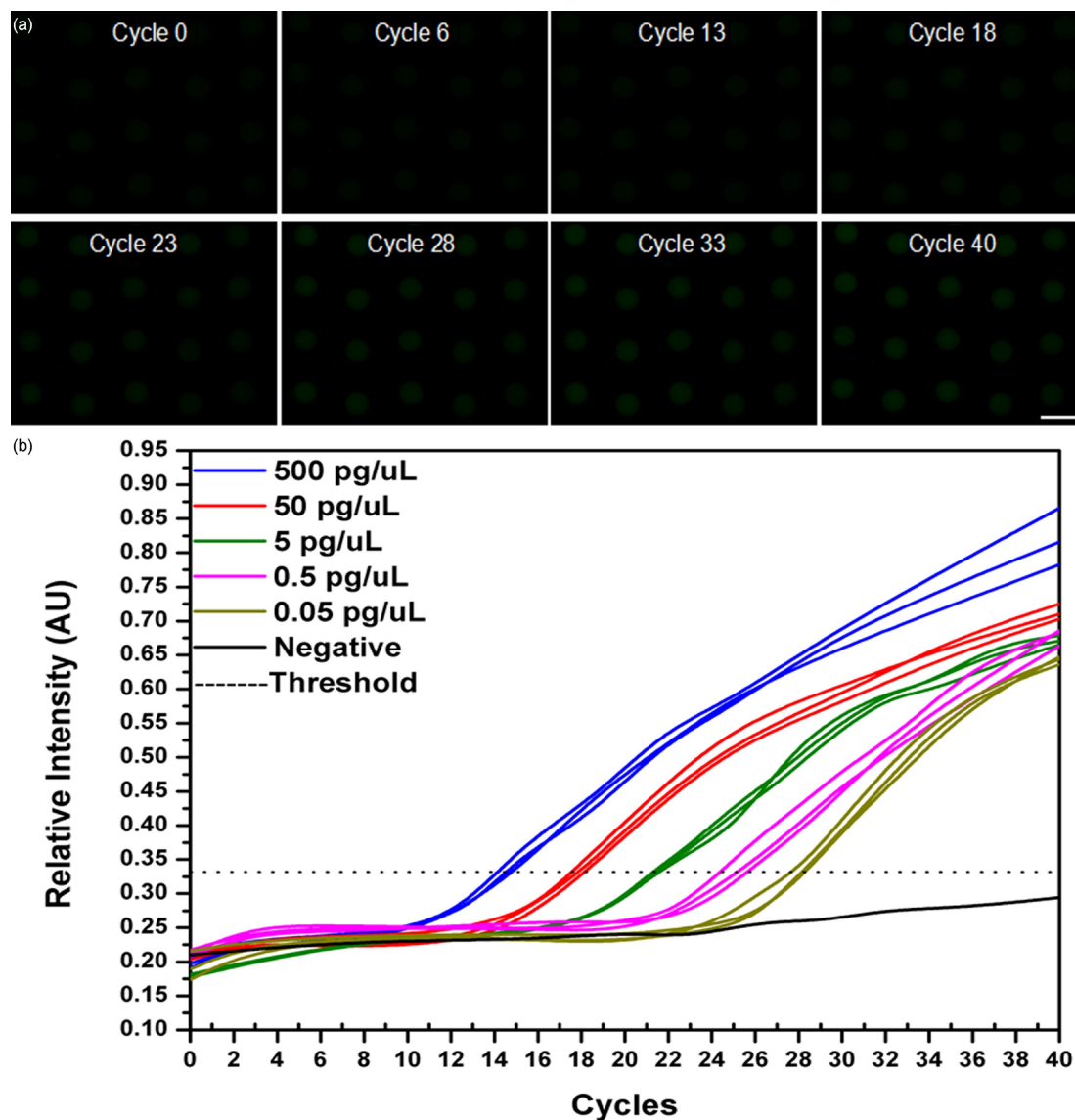


Fig. 5 Real-time PCR amplification of cDNA in droplets: (a) Fluorescence images of droplets with 50 pg/μL of cDNA as a function of thermal cycling. Scale bar: 200 μm. (b) Real-time amplification plots for a 1/10 dilution series of cDNA over five orders of magnitude. Threshold is 10 × the standard deviation of background. The lowest concentration amplified was 0.05 pg/μL, whose Ct was determined to be 28 ± 0.62.

This method has the advantages of high sensitivity and high-throughput compared with conventional real-time PCR systems. The picoliter droplet array can be readily applied to digital PCR and digital ELISA³⁹, with the potential to detect very low amounts of DNA and diagnostic genetic biomarkers down to the single-molecule level. In addition, it can also be useful for applications such as cell culture³⁸. Single bacterial cells could be cultured in the droplets to screen for resistant bacteria in the presence of a specific antibiotic, and subsequently collected for identification of the gene responsible for resistance. In the future, we will focus our research on optimizing the double-inkjet method for large-scale preparations and utilizing the picodroplet array for digital PCR applications.

Acknowledgements

This work was supported by grants from the Instrument Developing Project of the Chinese Academy of Sciences (Grant No. YZ201101 and YZ201301), the National Natural Science Foundation for Young Scholars (No.31200643) and Scientific and Technological Innovation “Interdiscipline and Cooperation Team” Project of Chinese Academy of Sciences, 2012. Prof. Jinling Yang is acknowledged for her support in the set-up of the inkjet printing system for droplet-in-oil fabrication. We are grateful to Qingquan Wei and Zhao Li for the technical assistance in the development of droplet-based PCR.

Notes and references

“State Key Laboratory on Integrated Optoelectronics, Institute of Semiconductors, Chinese Academy of Sciences. P.O. Box 912, Beijing, 100083, China.

^bJoint Laboratory of Bioinformation Acquisition and Sensing Technology, Institute of Semiconductors, Beijing Institute of Genomics, Chinese Academy of Sciences. P.O. Box 912, Beijing 100083, China.

*Corresponding author: Fax: +86-10-82305052; Tel: +86-10-82304979; Email: yudeyu@semi.ac.cn.

Electronic Supplementary Information (ESI) available:

Figure S1

Figure S2

Figure S3

Figure S4

Figure S5

Movie S1

Movie S2. See DOI: 10.1039/b000000x/

1. A. B. Theberge, F. Courtois, Y. Schaerli, M. Fischlechner, C. Abell, F. Hollfelder and W. T. Huck, *Angew. Chem. Int. Ed. Engl.*, 2010, **49**, 5846–5868.
2. M. A. Holden, D. Needham and H. Bayley, *J. Am. Chem. Soc.*, 2007, **129**, 8650–8655.
3. K. T. Kotz, Y. Gu and G. W. Faris, *J. Am. Chem. Soc.*, 2005, **127**, 5736–5737.
4. M. Chabert, K. D. Dorfman, P. de Cremoux, J. Roeraade and J. L. Viovy, *Anal. Chem.*, 2006, **78**, 7722–7728.
5. Z. Guttenberg, H. Muller, H. Habermuller, A. Geisbauer, J. Pipper, J. Felbel, M. Kielpinski, J. Scriba and A. Wixforth, *Lab Chip*, 2005, **5**, 308–317.
6. P. Neuzil, C. Zhang, J. Pipper, S. Oh and L. Zhuo, *Nucleic Acids Res.*, 2006, **34**, e77.
7. N. R. Bever, B. J. Hindson, E. K. Wheeler, S. B. Hall, K. A. Rose, I. M. Kennedy and B. W. Colston, *Anal. Chem.*, 2007, **79**, 8471–8475.
8. J. Pipper, M. Inoue, L. F.-P. Ng, P. Neuzil, Y. Zhang and L. Novak, *Nature Med.*, 2007, **13**, 1259–1263.
9. T. Thorsen, R. W. Roberts, F. H. Arnold and S. R. Quake, *Phys. Rev. Lett.*, 2001, **86**, 4163.
10. T. Nisisako, T. Torii and T. Higuchi, *Lab Chip*, 2002, **2**, 24.
11. D. R. Link, S. L. Anna, D. A. Weitz and H. A. Stone, *Phys. Rev. Lett.*, 2004, **92**, 054503.
12. S. L. Anna, N. Bontoux and H. A. Stone, *Appl. Phys. Lett.*, 2003, **82**, 364.
13. W. Du, L. Li, K. P. Nichols, and R.F. Ismagilov, *Lab Chip*, 2009, **9**, 2286–2292.
14. H. Wu, A. Wheeler and R. N. Zare, *Proc. Natl. Acad. Sci.*, 2004, **101**, 12809–12813.
15. L. Cai, N. Friedman and X. S. Xie, *Nature*, 2006, **440**, 358–362.
16. B. Huang, H. Wu, D. Bhaya, A. Grossman, S. Granier, B. K. Kobilka and R. N. Zare, *Science*, 2007, **315**, 81–84.
17. T. Thorsen, R. W. Roberts, F. H. Arnold and S. R. Quake, *Phys. Rev. Lett.*, 2001, **86**, 4163–4166.
18. K. A. Heyries, C. Tropini, M. VanInsberghe, C. Doolin, Oleh. I. Petriv, A. Singhal, K. Leung, C. B Hughesman and C. L. Hansen, *Nature Methods*, 2011, **8**, 649–651.
19. F. Shen, B. Sun, J. E. Kreutz, E. K. Davydova, W. Du, P. L. Reddy, L. J. Joseph and R.F. Ismagilov, *J. Am. Chem. Soc.*, 2011, **133**, 17705–17712.
20. J. E. Kreutz, T. Munson, T. Huynh, F. Shen, W. Du and R.F. Ismagilov, *Anal. Chem.*, 2011, **83**, 8158–8168.
21. S. Sakakihara, S. Araki, R. Iino and H. Noji, *Lab on Chip*, 2010, **10**, 3355–3362.
22. Z. Guttenberg, H. Muller, H. Habermuller, A. Geisbauer, J. Pipper, J. Felbel, M. Kielpinski, J. Scriba and A. Wixforth, *Lab Chip*, 2005, **5**, 308.
23. A. May, R. Kirchner, H. Muller, P. Hartmann, N. Hajj, A. Tresch, U. Zechner, W. Mann and T. Haaf, *Biol. Reprod.*, 2009, **80**, 194–202.
24. M. Kantelehner, R. Kirchner, P. Hartmann, J. W. Ellwart, M. Alunni-Fabbroni and A. Schumacher, *Nucleic Acids Res.*, 2011, **39**, E44–E68.
25. S. L. Angione, A. Chauhan and A. Tripathi, *Anal. Chem.*, 2012, **84**, 2654–2661.
26. H. Kim, S. Vishniakou and G. W. Faris, *Lab Chip*, 2009, **9**, 1230–1235.
27. U. Schmidt, S. Lutz-BOengel, H. Weisser, T. Sanger, S. Pollak, U. Schon, T. Zacher and W. Mann, *Int. J. Legal. Med.*, 2006, **120**, 42–48.
28. Y. Zhang, Y. Zhu, B. Yao and Q. Fang, *Lab Chip*, 2011, **11**, 1545–1549.
29. G. Arrabito, C. Galati, S. Castellano and B. Pignataro, *Lab Chip*, 2013, **13**, 68–72.
30. M. G. Pollack, R. B. Fair and A. D. Shenderov, *Appl. Phys. Lett.*, 2000, **77**, 1725–1726.
31. B. Hadwen, G. R. Broder, D. Morganti, A. Jacobs, C. Brown, J. R. Hector, Y. Kubota and H. Morgan, *Lab Chip*, 2012, **12**, 3305–3313.
32. N. Vergauwe, D. Witters, F. Ceyssens, S. Vermeir, B. Verbruggen, R. Puers and J. Lammertyn, *J. Micromech. Microeng.*, 2011, **21**, 054026–054036.
33. R. B. Fair, *Microfluidics and Nanofluidics*, 2007, **3**, 245–281.
34. MicroFab Technologies, <http://www.microfab.com/>, (accessed May 2014)
35. C. J. Beverung, C. J. Radke, H. W. Blanch, *Biophys. Chem.*, 1999, **81**, 59–80.
36. G. Arrabito, C. Galati, S. Castellano and B. Pignataro, *Lab Chip*, 2013, **13**, 68–72.
37. L. Li, D. Mustafı, Q. Fu, V. Tereshko, D. L. L. Chen, J. D. Tice and R. F. Ismagilov, *P. Natl. Acad. Sci. USA*, 2006, **103**, 19243–19248.
38. D. Bogojevic, M. D. Chamberlain, I. Barbulovic-Nad and A. R. Wheeler, *Lab Chip*, 2012, **12**, 627–634.
39. R. S. Sista, A. E. Eckhardt, V. Srinivasan, M. G. Pollack, S. Palanki and V. K. Pamula, *Lab Chip*, 2008, **8**, 2188–2196.
40. F. Shen, B. Sun, J. E. Kreutz, E. K. Davydova, W. Du, P. L. Reddy, L. J. Joseph and R. F. Ismagilov, *J Am Chem. Soc.*, 2011, **133**, 17705–17712.